AIP Applied Physics Letters

Mid-infrared time-domain ellipsometry: Application to Nb-doped SrTiO3

Andrea Rubano, Lukas Braun, Martin Wolf, and Tobias Kampfrath

Citation: Applied Physics Letters **101**, 081103 (2012); doi: 10.1063/1.4746263
View online: http://dx.doi.org/10.1063/1.4746263
View Table of Contents: http://scitation.aip.org/content/aip/journal/apl/101/8?ver=pdfcov
Published by the AIP Publishing

Mid-infrared time-domain ellipsometry: Application to Nb-doped $SrTiO_3$

Andrea Rubano,[a)] Lukas Braun, Martin Wolf, and Tobias Kampfrath
Fritz-Haber-Institut der Max-Planck-Gesellschaft, Berlin, Germany

(Received 8 June 2012; accepted 2 August 2012; published online 20 August 2012)

We present a method for determining the dielectric function of opaque materials precisely and reproducibly in the frequency range from 8 to 30 THz and higher. Our approach is based on measuring the polarization- and phase-resolved THz electrical transients reflected by the sample. This mid-infrared time-domain ellipsometry is applied to pure and Nb-doped strontium titanate $SrTiO_3$, which allows us to infer the longitudinal and transverse optical phonon frequencies and the free-carrier plasma frequency as a function of the charge carrier concentration. We extract and discuss the value of the effective mass of the charge carriers. © *2012 American Institute of Physics*. [http://dx.doi.org/10.1063/1.4746263]

The elusive terahertz (THz) frequency window extends from about 0.3 to 30 THz, thus covering the far-infrared (FIR) and lower part of the mid-infrared (MIR) spectral region. This window is of enormous interest for scientific and technical applications as it overlaps with many fundamental elementary excitations of physical systems, for instance molecular vibrations, phonons, quasi-free electrons, excitons, and magnons.[1,2] Sub-picosecond THz pulses can even be used to investigate the ultrafast dynamics of these resonances.[3] Moreover, the material-specific sensitivity makes THz radiation interesting for imaging and quality control.[4] In view of these applications, the accurate characterization of the optical response of a material at THz frequencies is important. This goal is usually realized with quasi-optical schemes in which the probing THz beam is transmitted through, or reflected off, the sample of interest. The maximum information that can be gained with such a linear probe is the complex-valued dielectric function ε and magnetic permeability μ of the sample material as a function of angular frequency ω. Unless magnetic resonances are present,[5] one has $\mu = 1$ to a very good approximation. The unambiguous determination of $\varepsilon(\omega)$ requires phase-sensitive detection schemes, most notably THz time-domain spectroscopy (THz-TDS),[2] which has been mainly conducted in transmission geometry.

In order to characterize opaque samples, THz-TDS has to be applied in reflection mode.[6–10] Conventional reflection-type THz-TDS measures the waveforms of the pulses reflected off the sample surface and a reference mirror. However, the position of sample and reference will be slightly different, leading to an altered beam path and systematic phase errors. Even more severe, changes in the beam direction will modify the overlap of THz beam and detector area and, thus, change the detector response. Both effects may significantly alter the THz conductivity extracted from the data. Therefore, a generally applicable measurement strategy is needed that makes the results independent of any instrumental function. Here, THz ellipsometry seems promising as it is self-referencing. It has been demonstrated in the 0.3-to-3 THz region,[6–9] yet the extension to higher, MIR frequencies remains to be shown.

In this letter, we report on an ellipsometric technique that is capable of measuring the dielectric function of opaque materials precisely and reproducibly in the frequency range from 8 to 30 THz. The scheme requires the measurement of the s and p polarization components of a THz wave reflected off the sample surface and a reference mirror. In contrast to conventional ellipsometry,[11] the coherent detection of the THz electric field provides the phase-information without the need to measure the reflected intensity as a function of the input polarization angle. We apply our approach to a prototype perovskite, pure and Nb-doped $SrTiO_3$ (STO:Nb) because STO:Nb has gained renewed attention for its peculiar electronic properties. Moreover, STO:Nb is an ideal benchmark sample since its numerous vibrational resonances give rise to reflectance modulations of almost 100%.

Figure 1(a) shows the scheme of a generic reflection-type THz-TDS experiment. A THz beam passes a wire-grid polarizer that selects either the polarization component along the s direction (perpendicular to the plane of incidence) or the p direction (within the plane of incidence and perpendicular to s). The beam is focused onto the sample surface, reflected, and after passing an analyzer, the transient electric field of the THz pulse is detected by electrooptic sampling. In the frequency domain, the resulting signal $S(\omega)$ at frequency $\omega/2\pi$ is given by the product

$$S = h_{\mathrm{d}} \boldsymbol{e}_\alpha \cdot \mathbf{P}_2 \mathbf{r} \mathbf{P}_1 \boldsymbol{E}^0. \tag{1}$$

Here, $\boldsymbol{E}^0(\omega) = {}^{\mathrm{t}}(E_p^0, E_s^0)$ denotes the complex-valued electric field amplitude after the polarizer, and the 2×2 Jones matrices $\mathbf{P}_1(\omega)$, $\mathbf{r}(\omega)$, and $\mathbf{P}_2(\omega)$ describe the propagation from the polarizer to the sample, the reflection off the sample, and the propagation from the sample to the analyzer. The unit vector $\boldsymbol{e}_\alpha = {}^{\mathrm{t}}(\cos\alpha, \sin\alpha)$ quantifies the analyzer which projects the THz field onto the analyzer direction $\boldsymbol{e}_\alpha$. Finally, $h_{\mathrm{d}}(\omega)$ embraces the beam propagation to the detector and the transfer function of the electrooptic sampling unit.[12] It is a scalar quantity as the polarization direction is fixed by the analyzer. Since the propagation through air (which is optically isotropic) does not depend on the polarization, the matrices $\mathbf{P}_{1,2}$ reduce to scalars $P_{1,2}$. We assume the sample is isotropic as well, such that $\mathbf{r}$ becomes diagonal with

[a)]Electronic mail: rubano@fhi-berlin.mpg.de.

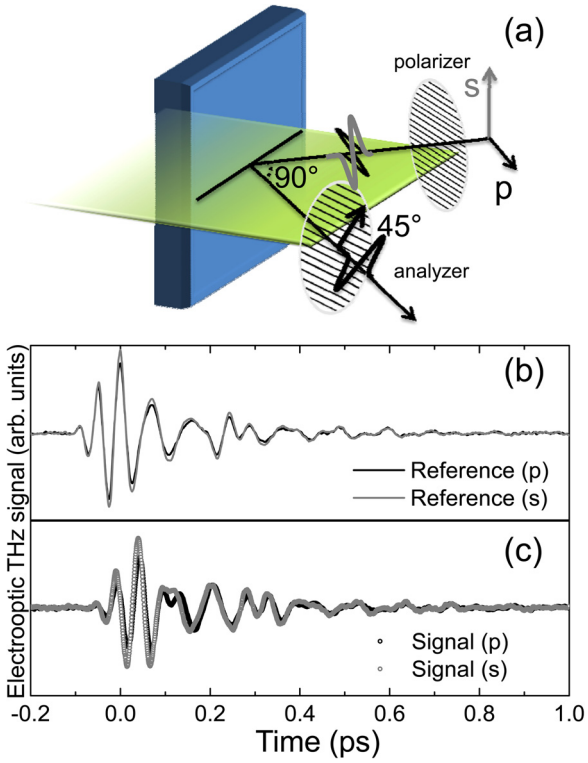

FIG. 1. (a) Scheme of our THz time-domain ellipsometer. The incoming polarization is set to either p or s polarization by means of a wire-grid polarizer. After reflection off the sample, the transient THz electric field is projected onto the 45° analyzer direction and finally detected by electrooptic sampling. (b) Typical p- and s-polarized THz waveforms after reflection off the gold reference mirror. (c) Same as (b) yet with the reference mirror replaced by an STO sample. The phase shift between sample and reference waves arises from a small sample displacement.

on-diagonal elements r_p and r_s. The electrooptic signals obtained for the polarizer set to p and s are then given by

$$S_j = h_{\mathrm{d}} e_{\alpha j} P_2 r_j P_1 E_j^0 \tag{2}$$

with $j = p$ or s. In a standard reflection measurement, one would choose either p- or s-polarized incident light and measure the signals $S_j(\omega)$ and $S_j^{\mathrm{ref}}(\omega)$ using the sample and a reference mirror, respectively. Taking the ratio. S_j/S_j^{ref} should then yield the sample reflectivity $r_j(\omega)$.

Note, however, that the surfaces of sample and reference mirror are not at perfectly the same position. This displacement will affect Eq. (2) via (i) modifications of $P_{1,2}$ due to path-length changes and (ii) modifications of h_{d} due to a different incidence of the THz pulse onto the 50 μm small sensitive area of the electrooptic detector. Thus, the cancelation of the transfer functions will be incomplete, leading to systematic errors in the determination of ε. As a consequence, alternative schemes have been suggested and demonstrated for the frequency range below 3 THz. Hirori *et al.*[13] made use of attenuated total internal reflection, where the sample material is probed by the evanescent THz field at the base of a prism. This method requires a perfect surface-matching between the prism and the sample, thus restricting its application to liquids and powders. Peiponen *et al.*[14] made use of a numerical method to correct for the unknown path-length change. Pashkin *et al.*[15] directed the THz pulse and the laser pulse used for electrooptic sampling along the same path, including the sample, which reduced phase errors due to (i) to ~1° at 1 THz. However, at MIR frequencies of 30 THz, the phase error will amount to ~30°, too large to achieve consistent results. Note that Refs. 14 and 15 deal with issue (i) whereas issue (ii) remains to be addressed.

For this purpose, we borrow concepts from ellipsometry and measure the signal for both p- and s-polarized incident light. Subsequent division cancels a great deal of the various transfer functions resulting in $S_p/S_s = (e_{\alpha p}/e_{\alpha s})(E_p^0/E_s^0)(r_p/r_s)$. We furthermore measure the ratio $S_p^{\mathrm{ref}}/S_s^{\mathrm{ref}}$ for a metallic reference mirror ($r_s = -r_p = 1$) to finally obtain the ellipsometric parameter,

$$\rho(\omega) = \tan\Psi \exp(\mathrm{i}\Delta) = \frac{r_p}{r_s} = -\frac{S_p}{S_s}\frac{S_s^{\mathrm{ref}}}{S_p^{\mathrm{ref}}}. \tag{3}$$

Here, we have defined the commonly used ellipsometric angels Ψ and Δ. Note that ρ contains mostly sample-intrinsic information. In case of an optically homogeneous and isotropic sample, the dielectric function can be determined using[10]

$$\varepsilon(\omega) = \sin^2\theta\left[1 + \left(\frac{1-\rho}{1+\rho}\right)^2 \tan^2\theta\right]. \tag{4}$$

Here, θ denotes the angle of incidence, and we have assumed the refractive index of air to be unity.

We now put our approach to test and apply it to Nb-doped STO whose narrow absorption features and large reflectance changes make it an ideal benchmark material. Beside this technical reason, STO and STO-based heterostructures have been attracting continuous scientific interest as they show numerous remarkable properties such as an insulator-to-metal transition.[16,17]

Our experimental setup [Fig. 1(a)] is composed as follows. We use 80% of the output of a Ti:sapphire laser oscillator (repetition rate 800 nm, pulse duration 10 fs, center wavelength 800 nm) to generate THz pulses by difference-frequency mixing in a 90 μm thick GaSe crystal.[18,19] We choose laser polarization and GaSe-crystal orientation such that the emitted THz pulses have an ≈45° polarization angle with respect to p and s directions. The THz beam is collimated and then focused onto the sample surface by means of two 90° off-axis parabolic mirrors. The THz polarization is set to p or s using a wire-grid polarizer (extinction ratio 10^4 from 0.7 to 50 THz). The polarizer angle with respect to the incidence plane is aligned by the aid of an auxiliary He-Ne laser beam. After transmission through the wire grid, several diffraction orders appear, and they all lie in the plane perpendicular to the wires. In this way, we determine the p and s directions with an accuracy of ±0.1°. The sample reflects the THz pulses under an angle of $\theta = 45° \pm 0.1°$. After the sample, a second wire-grid polarizer projects the reflected THz field onto an axis $\boldsymbol{e}_\alpha$, which lies $\alpha \approx 45°$ with respect to the incident plane. Setting this angle does not require particular accuracy as it does not show up in Eq. (3). Finally, the THz electric field is detected by electrooptic sampling in a 10 μm thick ZnTe (110) crystal.[19] Low-noise sampling of the electrooptic waveform is realized by a fast mechanical delay stage that scans a maximal delay range of 10 ps about 40 times per second.

We study as-received, commercial Nb-doped STO samples with a dopant density ranging from $N_d = 0$ (pure STO) to $2.1 \times 10^{20}\,\mathrm{cm}^{-3}$. The specimen are single-crystalline, (100)-oriented, 1 mm thick, and single-side polished. They exhibit a penetration depth of 1 μm or less over the whole frequency range of interest. Gold and silver mirrors are used as reference samples, and we do not observe any influence of this choice on our results.

Figures 1(b) and 1(c) display four typical THz waveforms which correspond to all combinations of sample/reference and *p*/*s* polarization configurations. We observe a significant temporal shift between the sample and reference curves. This delay arises from a change in the THz path length of only $\sim$10 μm that occurs when the sample is replaced by the reference mirror. In addition, we find amplitude variations of the THz signal of up to 10% when we unmount and remount the reference mirror (not shown). These variations arise from slight alterations of the path of the reflected beam leading to a different overlap of THz focus and sampled area of the detection crystal. We emphasize that both delay shift and changes in the detector response cancel in the normalization procedure of Eq. (3).

After Fourier transformation of the respective time-domain waveforms, we obtain the sample and reference power spectra for *p*-polarized pulses [Fig. 2(a)]. They cover the very broad frequency range from 8 to 30 THz, and the sample spectrum exhibits a pronounced minimum at about 14 THz. Despite the detector response $h_d(\omega)$ may differ for both measurements (see above), we divide sample and reference spectra to obtain an approximate reflectance spectrum, $|r_p(\omega)|^2 \approx |S_p/S_p^{\mathrm{ref}}|^2$, which is shown in Fig. 2(b) for samples having different dopant density N_d. The overall appearance of these spectra is consistent with those measured by conventional infrared spectroscopy without phase resolution.[20,21] In case of pure STO, the reststrahlen band featuring high reflectance is embraced by the minima at 14.9 and 25.1 THz. For $N_d > 1.5 \times 10^{20}\,\mathrm{cm}^{-3}$, the shape of the reflectance spectra changes drastically because the plasma frequency of the free charge carriers crosses the spectral window investigated.

Using Eq. (3) and the experimental data of Fig. 1, we obtain the ellipsometric angles Ψ and Δ, an example of which is shown in Fig. 3(a). The angle $\Psi - 45^\circ$ represents the difference of the sample's efficiency to reflect *p*- and *s*-polarized light [Eq. (3)], whereas Δ is the phase-shift difference of the two polarization components. Accordingly, Ψ and Δ, respectively, exhibit a rather peak-like structure at 15 THz and its derivative, indicating a resonance. Note that the curves of Fig. 3(a) are an average of eight subsequent measurement cycles, each involving a change from sample to reference mirror and back. We emphasize that the size of the resulting error bars [Fig. 3(a)] is much smaller than the variation of Ψ and Δ over the frequency window considered, which demonstrates that our method provides robust and reproducible results.[22] Note that the maximum error of the

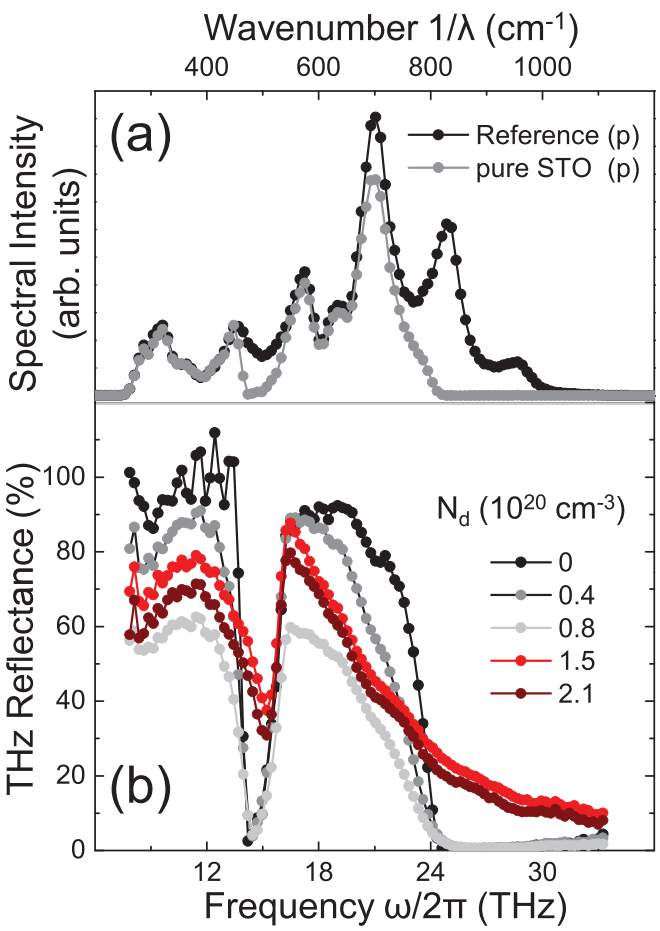

FIG. 2. (a) Power spectra of the *p*-polarized THz pulses reflected from pure STO and reference mirror. (b) Approximate *p*-polarization reflectance spectra of Nb:STO at various Nb-dopant densities N_d.

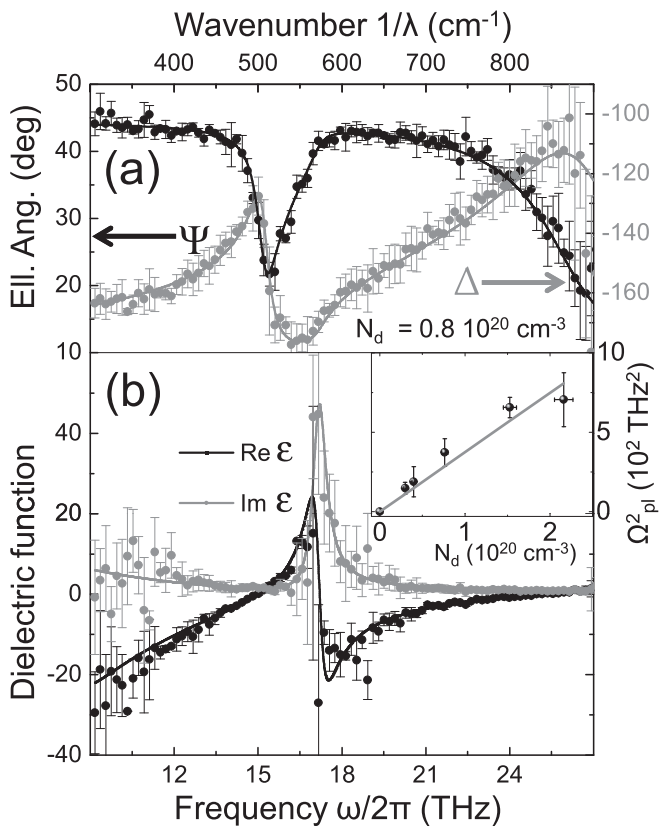

FIG. 3. (a) Measured ellipsometric angles Ψ and Δ at $N_d = 0.8 \times 10^{20}\,\mathrm{cm}^{-3}$. Error bars are the result of eight repeated measurements, each including a change between sample and reference mirror. (b) Real and imaginary part of the dielectric function as extracted from the data of (a) using Eq. (4). Solid lines represent a model fit with Eq. (5). Inset: extracted squared plasma frequency Ω_{pl}^2 versus dopant density N_d. Solid line is a linear fit.

TABLE I. Values of LO and TO phonon frequencies of pure STO extracted from this experiment along with literature values. The obtained $\varepsilon_\infty = 5.6 \pm 1$ is in agreement with Ref. 25.

Phonon mode	Frequency (THz)	Ref. 21	Ref. 25
LO1	5.57 ± 1.7	5.90	5.06
TO1	2.99 ± 0.9	3.41	2.88
LO2	14.89 ± 0.09	14.98	14.00
TO2	7.04 ± 1.7	6.00	5.21
LO3	25.09 ± 0.84	24.61	23.65
TO3	17.03 ± 0.48	17.05	16.07

phase difference Δ corresponds to a propagation length of only $\sim$250 nm at a frequency of 20 THz. This error most likely arises from length drifts of THz and gate-beam paths between subsequent p- and s-type measurements. It could be further reduced by faster switching the polarizer between p and s settings.

We now apply Eq. (4) to the ellipsometric data of Fig. 3(a) and finally arrive at the desired dielectric function ε [Fig. 3(b)]. We find a resonance structure at 17 THz that can be identified as an optical phonon.[21] All other infrared-active STO phonon modes are present in the obtained $\varepsilon(\omega)$ as well. In particular, the very strong soft mode at $\approx$2.8 THz shows up as a long tail that can be seen below 12 THz in all samples, including insulating pure STO. To be more quantitative, the measured ellipsometric angles Ψ and Δ are fit using Eq. (3) and the model dielectric function[21]

$$\varepsilon = \varepsilon_\infty \prod_{j=1}^{3} \frac{\Omega_{j\mathrm{LO}}^2 - \omega^2 + \mathrm{i}\Gamma_{j\mathrm{LO}}\omega}{\Omega_{j\mathrm{TO}}^2 - \omega^2 + \mathrm{i}\Gamma_{j\mathrm{TO}}\omega} - \frac{\Omega_{\mathrm{pl}}^2}{\omega^2 - \mathrm{i}\Gamma\omega}. \quad (5)$$

Here, the first term is a product whose zeros correspond to three longitudinal-optical (LO) phonon modes (frequency $\Omega_{j\mathrm{LO}}$ and damping rate $\Gamma_{j\mathrm{LO}}$) whereas the poles represent the three transverse-optical (TO) phonons ($\Omega_{j\mathrm{TO}}$ and $\Gamma_{j\mathrm{TO}}$). The second, Drude-type term quantifies the contribution of the free-charge carriers (plasma frequency Ω_{pl} and scattering rate Γ). The various phonon frequencies and their error as obtained from the fit procedure are summarized in Table I for pure STO ($N_\mathrm{d} = 0$), along with values from existing literature. We find good agreement between our measurements and previous work. The errors indicate that phonon frequencies within the frequency range covered by our THz source can be measured with an accuracy of $\sim$1 % whereas resonance frequencies outside this range have a $\sim$20 % uncertainty.

We finally consider the extracted squared plasma frequency Ω_{pl}^2 that is found to increase approximately linearly with the dopant density N_d (inset of Fig. 3). Indeed, assuming that at room temperature each Nb atom donates one electron, the plasma frequency is given by $\Omega_{\mathrm{pl}}^2 = e^2 N_\mathrm{d}/\varepsilon_0 m^*$ where m^* is the effective mass of the free charge carriers, and ε_0 is the vacuum dielectric constant. A linear fit to the measured Ω_{pl}^2 versus N_d then yields $m^* = (21.5 \pm 2.4) m_\mathrm{e}$ where m_e is the free-electron mass. Similar values have been predicted[23] ($16 m_\mathrm{e}$) and measured by Hall probes[24] ($15 m_\mathrm{e}$). Such high masses may point to polaronic behavior of the electrons.[23,24]

In conclusion, we have demonstrated robust and reliable measurements of the dielectric function of opaque materials at MIR frequencies from 8 to 30 THz using time-domain ellipsometry in reflection mode. Our technique is based on electrooptic sampling of the transient electric field of the p and s polarization components of a THz pulse. Statistical errors can be further reduced by faster and automated switching between the p and s polarization and by varying the angle of incidence. Note that our approach could be implemented in other schemes such as Fourier transform infrared (FTIR) spectrometers whose interferometric time-domain detection also allows for phase-resolved measurements. Finally, as our setup employs sub-picosecond THz pulses, it is an ideal tool to probe the temporal dynamics of the dielectric function of a photoexcited opaque sample in a pump-probe scheme.[3,11]

We acknowledge A. Marino, U. Scotti di Uccio, and V. Cataudella, from the University of Naples Federico II, for the fruitful discussions.

[1] M. Hangyo, M. Tani, and T. Nagashima, Int. J. Infrared Millim. Waves **26**, 12 (2005).
[2] M. Tonouchi, Nature Photon. **1**, 99 (2007).
[3] R. Ulbricht, E. Hendry, J. Shan, T. F. Heinz, and M. Bonn, Rev. Mod. Phys. **83**, 543–586 (2011).
[4] B. Ferguson and X.-C. Zhang, Nature Mater. **1**, 26–33 (2002).
[5] D. R. Smith, S. Schultz, P. Markoš, and C. M. Soukoulis, Phys. Rev. B **65**, 195104 (2002).
[6] T. Nagashima and M. Hangyo, Appl. Phys. Lett. **79**, 3917 (2001).
[7] K. Yatsugi, N. Matsumoto, T. Nagashima, and M. Hangyo, Appl. Phys. Lett. **98**, 212108 (2011).
[8] Y. Ino, R. Shimano, Y. Svirko, and M. Kuwata-Gonokami, Phys. Rev. B **70**, 155101 (2004).
[9] N. Matsumoto, T. Hosokura, T. Nagashima, and M. Hangyo, Opt. Lett. **36**, 265 (2011).
[10] A. Pashkin, M. Porer, M. Beyer, K. W. Kim, A. Dubroka, C. Bernhard, X. Yao, Y. Dagan, R. Hackl, A. Erb, J. Demsar, R. Huber, and A. Leitenstorfer, Phys. Rev. Lett. **105**, 067001 (2010).
[11] R. M. A. Azzam and N. M. Bashara, *Ellipsometry and Polarized Light* (North Holland, 1988).
[12] T. Kampfrath, J. Nötzold, and M. Wolf, Appl. Phys. Lett. **90**, 231113 (2007).
[13] H. Hirori, K. Yamashita, M. Nagai, and K. Tanaka, Jpn. J. Appl. Phys. **43**, L1287 (2004).
[14] K.-E. Peiponen, E. Gornov, Y. Svirko, Y. Ino, M. Kuwata-Gonokami, and V. Lucarini, Phys. Rev. B **72**, 245109 (2005).
[15] A. Pashkin, M. Kempa, H. Němec, F. Kadlec, and P. Kužel, Rev. Sci. Instrum. **74**, 4711 (2003).
[16] A. Ohtomo and H. Y. Hwang, Nature **427**, 423 (2004).
[17] A. Rubano, M. Fiebig, D. Paparo, A. Marino, D. Maccariello, U. Scotti di Uccio, F. Miletto Granozio, L. Marrucci, C. Richter, S. Paetel, and J. Mannhart, Phys. Rev. B **83**, 155405 (2011).
[18] R. A. Kaindl, D. C. Smith, M. Joschko, M. P. Hasselbeck, M. Woerner, and T. Elsaesser, Opt. Lett. **23**, 861–863 (1998).
[19] R. Huber, A. Brodschelm, F. Tauser, and A. Leitenstorfer, Appl. Phys. Lett. **76**, 3191 (2000).
[20] J. L. Servoin, Y. Luspin, and F. Gervais, Phys. Rev. B **22**, 5501 (1980).
[21] F. Gervais, J. L. Servoin, A. Baratoff, J. G. Bednorz, and G. Binnig, Phys. Rev. B **47**, 8187 (1993).
[22] A small deviation $\Delta\varphi \sim 0.1°$ of the polarizer axis from s or p directions leads (to first order) to an error $\Delta\rho = (1 - \rho^2)\Delta\varphi$ of the ellipsometric parameter. In our experiment, we have approximately $|\rho| > 0.3$ implying $|\Delta\rho/\rho| < 0.2\%$. This systematic error is negligible with respect to the statistical errors.
[23] J. F. Scott, A. Q. Jiang, S. A. T. Redfern, M. Zhang, and M. Dawbera, J. Appl. Phys. **94**, 3333 (2003).
[24] H. P. R. Frederikse, W. R. Thurber, and W. R. Hosler, Phys. Rev. **134**, A442 (1964).
[25] J. T. Devreese, S. N. Klimin, J. L. M. van Mechelen, and D. van der Marel, Phys. Rev. B **81**, 125119 (2010).